



1 Microbial functional signature in the atmospheric boundary layer

2

3 Romie Tignat-Perrier^{1,2*}, Aurélien Dommergue¹, Alban Thollot¹, Olivier Magand¹, Timothy
4 M. Vogel², Catherine Larose²

5

6 ¹Institut des Géosciences de l'Environnement, Université Grenoble Alpes, CNRS, IRD,
7 Grenoble INP, Grenoble, France

8 ²Environmental Microbial Genomics, Laboratoire Ampère, École Centrale de Lyon, Université
9 de Lyon, Écully, France

10

11 Correspondence to: Romie Tignat-Perrier (romie.tignat-perrier@univ-grenoble-alpes.fr)

12

13 Abstract

14 Microorganisms are ubiquitous in the atmosphere and some airborne microbial cells were
15 shown to be particularly resistant to atmospheric physical and chemical conditions (*e.g.*, UV
16 radiation, desiccation, presence of radicals). In addition to surviving, some cultivable
17 microorganisms of airborne origin were shown to be able to grow on atmospheric chemicals in
18 laboratory experiments. Metagenomic investigations have been used to identify specific
19 signatures of microbial functional potential in different ecosystems. We conducted a
20 preliminary comparative metagenomic study on the overall microbial functional potential and
21 specific metabolic and stress-related microbial functions of atmospheric microorganisms in
22 order to determine whether airborne microbial communities possess an atmosphere-specific
23 functional potential signature as compared to other ecosystems (*i.e.* soil, sediment, snow, feces,
24 surface seawater *etc.*). In absence of a specific atmospheric signature, the atmospheric samples
25 collected at nine sites around the world were similar to their underlying ecosystems. In addition,
26 atmospheric samples were characterized by a relatively high proportion of fungi. The higher
27 proportion of sequences annotated as genes involved in stress-related functions (*i.e.* functions
28 related to the response to desiccation, UV radiation, oxidative stress *etc.*) resulted in part from
29 the high concentrations of fungi that might resist and survive atmospheric physical stress better
30 than bacteria.

31

32 **Keywords:** atmospheric microorganisms, airborne microbial communities, planetary boundary
33 layer, metagenomic sequencing, comparative metagenomics, selective processes

34

35 1 Introduction

36 Microorganisms are ubiquitous in the atmosphere and reach concentrations of up to 10⁶
37 microbial cells per cubic meter of air (Tignat-Perrier et al., 2019). Due to their important roles
38 in public health and meteorological processes (Ariya et al., 2009; Aylor, 2003; Brown and
39 Hovmöller, 2002; Delort et al., 2010; Griffin, 2007), understanding how airborne microbial
40 communities are distributed over time and space is critical. While the concentration and
41 taxonomic diversity of airborne microbial communities in the planetary boundary layer have
42 recently been described (Els et al., 2019; Innocente et al., 2017; Tignat-Perrier et al., 2019), the
43 functional potential of airborne microbial communities remains unknown. Most studies have
44 focused on laboratory cultivation to identify possible metabolic functions of microbial strains
45 of atmospheric origin, mainly from cloud water (Amato et al., 2007; Ariya et al., 2002; Hill et
46 al., 2007; Vaitilingom et al., 2010, 2013). Given that cultivatable organisms represent about 1
47 % of the entire microbial community (Vartoukian et al., 2010), culture-independent techniques
48 and especially metagenomic studies applied to atmospheric microbiology have the potential to
49 provide additional information on the selection and genetic adaptation of airborne



50 microorganisms. However, to our knowledge, only five metagenomic studies on airborne
51 microbial communities at one or two specific sites per study exist (Aalismail et al., 2019; Amato
52 et al., 2019; Cao et al., 2014; Gusareva et al., 2019; Yooseph et al., 2013). Metagenomic
53 investigations of complex microbial communities in many ecosystems (for example, soil,
54 seawater, lakes, feces, sludge) have provided evidence that microorganism functional
55 signatures reflect the abiotic conditions of their environment, with different relative abundances
56 of specific microbial functional classes (Delmont et al., 2011; Li et al., 2019; Tringe et al., 2005;
57 Xie et al., 2011). This observed correlation of microbial community functional potential and
58 the physical and chemical characteristics of their environments could have resulted from genetic
59 modifications (microbial adaptation) (Brune et al., 2000; Hindré et al., 2012; Rey et al., 2016;
60 Yooseph et al., 2010) and/or physical selection. The latter refers to the death of sensitive cells
61 and the survival of resistant or previously adapted cells. This physical selection can occur when
62 microorganisms are exposed to physiologically adverse conditions.

63 The presence of a specific microbial functional signature in the atmosphere has not been
64 investigated yet. Microbial strains of airborne origin have been shown to survive and develop
65 under conditions typically found in cloud water (*i.e.* high concentrations of H₂O₂, typical cloud
66 carbonaceous sources, UV radiation *etc.*) (Amato et al., 2007; Joly et al., 2015; Vařtilingom et
67 al., 2013). While atmospheric chemicals might lead to some microbial adaptation, physical and
68 unfavorable conditions of the atmosphere such as UV radiation, low water content and cold
69 temperatures might select which microorganisms can survive in the atmosphere. From the pool
70 of microbial cells being aerosolized from Earth's surfaces, these adverse conditions might act
71 as a filter in selecting cells already resistant to unfavorable physical conditions. Fungal cells
72 and especially fungal spores might be particularly adapted to survive in the atmosphere due to
73 their innate resistance (Huang and Hull, 2017) and might behave differently than bacterial cells.
74 Still, the proportion and nature (*i.e.* fungi versus bacteria) of microbial cells that are resistant to
75 the harsh atmospheric conditions within airborne microbial communities are unknown.

76 Our objective was to determine whether airborne microorganisms in the planetary boundary
77 layer possess a specific functional signature as compared to other ecosystems since this might
78 indicate that microorganisms with specific functions tend to be more aerosolized and/or
79 undergo a higher survival in this environment. Our previous study showed that airborne
80 microbial taxonomy mainly depends on the underlying ecosystems, indicating that the local
81 environments are the main source of airborne microorganisms (Tignat-Perrier et al., 2019). Still,
82 we do not know if airborne microbial communities result from random or specific
83 aerosolization of the underlying ecosystems' microorganisms. We used a metagenomic
84 approach to compare the differences and similarities of both the overall functional potential and
85 specific microbial functions (metabolic and stress-related functions) between microbial
86 communities from the atmosphere and other ecosystems (soil, sediment, surface seawater, river
87 water, snow, human feces, phyllosphere and hydrothermal vent). We sampled airborne
88 microbial communities at nine different locations around the world during several weeks to get
89 a global-scale view and to capture the between and within-site variability in atmospheric
90 microbial functional potential.

91

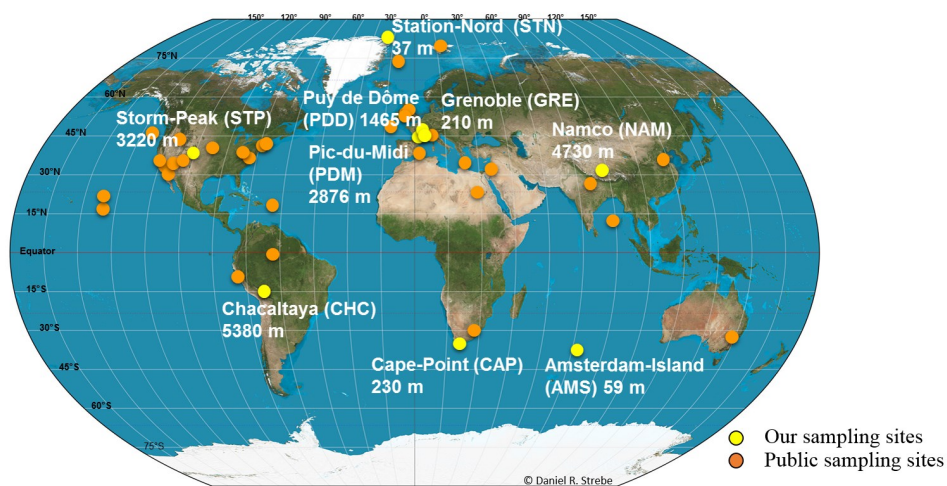
92 **2 Material and Methods**

93 **2.1 Sites and sampling**

94 Air samples were collected at nine sites in 2016 and 2017. Sites were characterized by different
95 latitudes (from the Arctic to the sub-Antarctica; **Fig 1**), elevations from sea level (from 59 m to
96 5230 m; **Fig 1**) and environment type (from marine for Amsterdam-Island or AMS, to coastal
97 for Cape Point or CAP, polar for Station Nord or STN and terrestrial for Grenoble or GRE,
98 Chacaltaya or CHC, puy de Dôme or PDD, Pic-du-Midi or PDM, Storm-Peak or STP and
99 Namco or NAM - **Table S1**). The number of samples collected per site varied from seven to



100 sixteen (**Table S1**). We collected particulate matter smaller than 10 μm (PM₁₀) on quartz fiber
101 filters (5.9'' round filter and 8'' \times 10'' rectangular types) using high volume air samplers
102 (TISCH, DIGITEL, home-made) installed on roof tops or terraces (roughly 10 m above ground
103 level). To avoid contamination, quartz fiber filters as well as all the material in contact with the
104 filters (*i.e.* filter holders, aluminium foils and plastic bags in which the filters were transported)
105 were sterilized using strong heating (500 °C for 8 h) and UV radiation, respectively as detailed
106 in Dommergue et al., 2019. The collection time per sample lasted one week, and the collected
107 volumes ranged from 2000 m³ to 10000 m³ after standardization using SATP standards
108 (Standard Ambient Pressure and Temperature). Detailed sampling protocols including negative
109 control filters are presented in Dommergue et al. 2019. MODIS (Moderate resolution imaging
110 spectroradiometer) land cover approach (5' \times 5' resolution) (Friedl et al., 2002; Shannan et al.,
111 2014) was used to quantify landscapes in the 50 km diameter area of our nine sampling sites
112 (**Fig S1**).
113
114



115
116 **Fig 1. Sample collection locations.** Map showing the geographical location and elevation from
117 sea level of our nine sampling sites (in yellow), and the geographical position of whose public
118 metagenomes come from (in orange). Abbreviations of our nine sampling sites are indicated in
119 brackets.

120
121 **2.2 Molecular biology analyses**

122 **2.2.1 DNA extraction**

123 DNA was extracted from three circular pieces (punches) from the quartz fiber filters (diameter
124 of one punch: 38 mm) using the DNeasy PowerWater kit with some modifications as detailed
125 in Dommergue et al., 2019. During cell lysis, the PowerBead tube containing the three punches
126 and the pre-heated lysis solution were heated at 65 °C during one hour after a 10-min vortex
127 treatment at maximum speed. We then separated the filter debris from the lysate by
128 centrifugation at 1000 rcf for 4 min. From this step on, we followed the DNeasy PowerWater
129 protocol. DNA concentration eluted in 100 μL of buffer was measured using the High Sensitive
130 Qubit Fluorometric Quantification (Thermo Fisher Scientific). DNA was stored at -20 °C.

131
132 **2.2.2 Real-Time qPCR analyses**



133 **16S rRNA gene qPCR.** The bacterial cell concentration was approximated by the number of
134 16S rRNA gene copies per cubic meter of air. The V3 region of the 16S rRNA gene was
135 amplified using the SensiFast SYBR No-Rox kit (Bioline) and the following primers sequences:
136 Eub 338f 5'-ACTCCTACGGGAGGCAGCAG-3' as the forward primer and Eub 518r 5'-
137 ATTACCGCGGCTGCTGG-3' as the reverse primer (Fierer et al., 2005) on a Rotorgene 3000
138 machine (Qiagen). The reaction mixture of 20 μ L contained 10 μ L of SYBR master mix, 2 μ L
139 of DNA and RNase-free water to complete the final 20 μ L volume. The qPCR 2-step program
140 consisted of an initial step at 95 °C for 2 min for enzyme activation, then 35 cycles of 5 s at 95
141 °C and 20 s at 60 °C hybridization and elongation. A final step was added to obtain a
142 denaturation from 55 °C to 95 °C with increments of 1 °C s⁻¹. The amplicon length was around
143 200 bp. PCR products obtained from DNA from a pure culture of *Escherichia coli* were cloned
144 in a plasmid (pCRTM2.1-TOPO® vector, Invitrogen) and used as standard after quantification
145 with the Broad-Range Qubit Fluorometric Quantification (Thermo Fisher Scientific).

146 **18S rRNA gene qPCR.** The fungal cell concentration was estimated by the number of 18S
147 rRNA gene copies per cubic meter of air. The region located at the end of the SSU 18S rRNA
148 gene, near the ITS 1 region, was quantified using the SensiFast SYBR No-Rox kit (Bioline)
149 and the following primers sequences: FR1 5'-AICCATTCAATCGGTAIT-3' as the forward
150 primer and FF390 5'-CGATAACGAACGAGACCT-3' as the reverse primer (Chemidlin
151 Prévost-Bouré et al., 2011) on a Rotorgene 3000 machine (Qiagen). The reaction mixture of 20
152 μ L contained 10 μ L of SYBR master mix, 2 μ L of DNA and RNase-free water to complete the
153 final 20 μ L volume. The qPCR 2-steps program consisted of an initial step at 95 °C for 5 min
154 for enzyme activation, then 35 cycles of 15 s at 95 °C and 30 s at 60 °C hybridization and
155 elongation. A final step was added to obtain a denaturation from 55 °C to 95 °C with increments
156 of 1 °C s⁻¹. The amplicon length was around 390 bp. PCR products obtained from DNA from a
157 soil sample were cloned in a plasmid (pCRTM2.1-TOPO® vector, Invitrogen) and used as
158 standard after quantification with the Broad-Range Qubit Fluorometric Quantification (Thermo
159 Fisher Scientific).

160

161 2.2.3 MiSeq Illumina metagenomic sequencing

162 **Metagenomic library preparation.** Metagenomic libraries were prepared from 1 ng of DNA
163 using the Nextera XT Library Prep Kit and indexes following the protocol in Illumina's
164 "Nextera XT DNA Library Prep Kit" reference guide with some modifications for samples with
165 DNA concentrations below 1 ng as follows. The tagmented DNA was amplified over 13 PCR
166 cycles instead of 12 PCR cycles, and the libraries (after indexing) were resuspended in 30 μ L
167 of RBS buffer instead of 52.5 μ L. Metagenomic sequencing was performed using the MiSeq
168 and V2 technology of Illumina with 2 x 250 cycles. At the end of the sequencing, the adapter
169 sequences were removed by internal Illumina software.

170 **Reads quality filtering.** Reads 1 and reads 2 per sample were not paired but merged in a
171 common file before filtering them based on read quality using the tool FASTX-Toolkit
172 (http://hannonlab.cshl.edu/fastx_toolkit/) using a minimum read quality of Q20, minimum read
173 length of 120 bp and one maximum number of N per read. Samples with less than 6000 filtered
174 sequences were removed from the dataset.

175

176 2.2.4 Downloading of public metagenomes

177 Public metagenomes were downloaded from the MGRAST and SRA (NCBI) databases as
178 quality filtered read-containing fasta files and raw read containing fastq files, respectively. The
179 fastq files containing raw reads underwent the same quality filtering as our metagenomes (as
180 discussed above). The list of the metagenomes, type of ecosystem, number of sequences and
181 sequencing technology (*i.e.* MiSeq, HiSeq or 454) are summarized in **Table S2**. The sampling
182 sites are positioned on the map in **Fig 1**.



183

184 **2.3 Data analyses**

185 All graphical and multivariate statistical analyses were carried out using the vegan (Oksanen et
186 al., 2019), ggplot2 (Hadley and Winston, 2019) and reshape2 (Wickham, 2017) packages in the
187 R environment (version 3.5.1).

188

189 **2.3.1 Annotation of the metagenomic reads**

190 Firstly, to access the overall functional potential of each sample, the filtered sequences per
191 sample were functionally annotated using Diamond, then the gene-annotated sequences were
192 grouped in the different SEED functional classes (around 7000 functional classes, referred
193 simply to as functions) using MEGAN version 6 (Huson et al., 2009). Functional classes that
194 were present ≤ 2 times in a sample were removed of this sample. In parallel, the Kraken software
195 (Wood and Salzberg, 2014) was used to retrieve the bacterial and fungal sequences separately
196 from the filtered sequences using the Kraken bacterial database and FindFungi (Donovan et al.,
197 2018) fungal database (both databases included complete genomes), respectively (and using
198 two different runs of Kraken). Separately, both the bacterial and fungal sequences were also
199 functionally annotated using Diamond and MEGAN version 6 (number of sequences
200 functionally annotated in **Table S3**).

201 Secondly, for specific metabolic and stress-related functions, we annotated the sequences using
202 eggNOG-Mapper version 1 (Diamond option), then examined specific GO (Gene Ontology)
203 terms chosen based on their importance for microbial resistance to atmospheric-like conditions.
204 The different GO terms used were the following: GO:0042744 (hydrogen peroxide catabolic
205 activity), GO:0015049 (methane monooxygenase activity) as specific metabolic functions and
206 GO:0043934 (sporulation), GO:0009650 (response to UV), GO:0034599 (cell response to
207 oxidative stress), GO:0009269 (response to desiccation) as stress-related functions. The number
208 of hits of each GO term was normalized per 10000 annotated sequences and calculated from all
209 sequences, bacterial sequences and fungal sequences for each sample. The number of sequences
210 annotated by eggNOG-Mapper (Huerta-Cepas et al., 2017) was also evaluated (**Table S3**). The
211 putative concentration of a specific function or functional class in the samples is determined as
212 the concentration of sequences annotated as one of the functional proteins associated to this
213 function (or functional class).

214

215 **2.3.2 Statistical analyses**

216 Observed functional richness and evenness were calculated per sample after rarefaction on all
217 sequences (rarefaction at 2000 sequences), bacterial sequences (rarefaction at 500 sequences)
218 and fungal sequences (rarefaction at 500 sequences). The distribution of the samples was
219 analyzed based on the SEED functional classes (using all sequences). PCoA and hierarchical
220 clustering analysis (average method) were carried out on the Bray-Curtis dissimilarity matrix
221 based on the relative abundances of the different SEED functional classes. SIMPER analyses
222 were used to identify the functions responsible for the clustering of samples in groups. Because
223 of the non-normality of the data, Kruskal-Wallis analyses (non-parametric version of ANOVA)
224 and Dunn's post-hoc tests were used to test the difference between the percentage of fungal
225 sequences as well as the number of hits of each Gene Ontology term (normalized per 10000
226 annotated sequences) among the different sites and the different ecosystems.

227

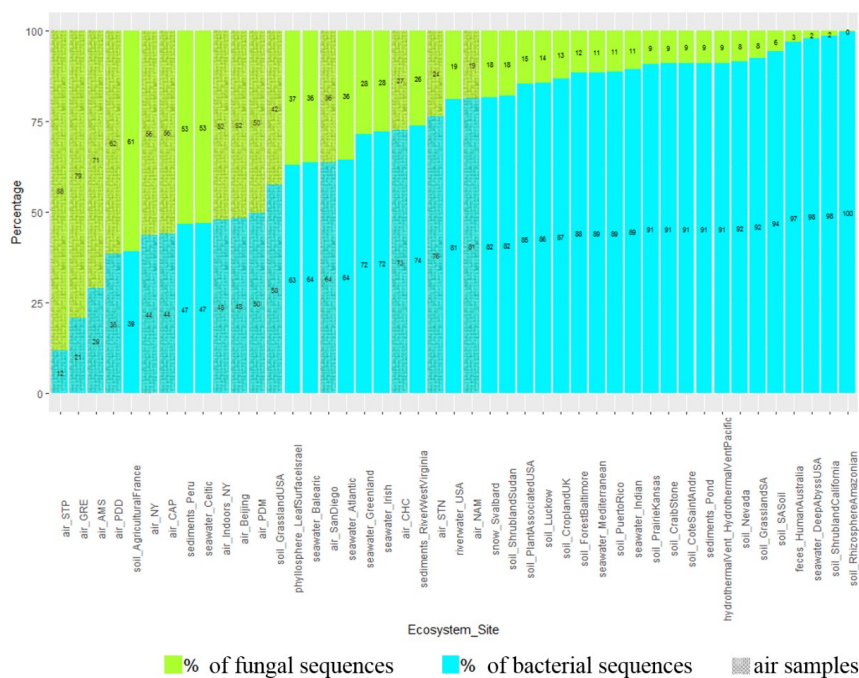
228 **3 Results**

229 **3.1 Percentage of fungal sequences**

230 The percentage of sequences annotated as belonging to fungal genomes (or fungal sequences,
231 as opposed to bacterial sequences) was on average higher in air samples compared to soil ($P < 10^{-5}$),
232 snow ($P = 10^{-3}$), seawater ($P = 0.03$) and sediment samples ($P = 10^{-3}$; **Fig 2** and **Table S4**).



233 Among the air samples, NAM (19%), STN (24%) and CHC (27%) showed the lowest
 234 percentages of fungal sequences on average while STP (88%), GRE (79%), AMS (71%) and
 235 PDD (62%) showed the highest percentages. For the ecosystems that were only represented by
 236 one sample, and therefore, were not evaluated by the Kruskal-Wallis test, we observed average
 237 percentages of fungal reads of 3% in feces, 9% in hydrothermal vents, 19% in river water
 238 samples and 37% in the phyllosphere. Some samples from soil, sediments and seawater such as
 239 French agricultural soil (61%), Peru sediments (53%) and Celtic seawater (53%) had relatively
 240 high percentages of fungal sequences while other samples had less than 50%. The number of
 241 fungal and bacterial cells was also estimated using 16S rRNA and 18S rRNA gene copy
 242 numbers per cubic meter of air, respectively. qPCR results on air samples are available in
 243 Tignat-Perrier et al., 2019. Air samples had ratios between bacterial cell and fungal cell
 244 concentrations from around 4.5 times up to 160 times lower than soil samples (**Table S4**).
 245
 246



247

248 **Fig 2. Percentage of fungal and bacterial sequences in the metagenomes.** The percentages
 249 are established as the number of sequences annotated as belonging to fungal and bacterial
 250 genomes over the sum of bacterial and fungal sequences in the metagenomes. The mean was
 251 calculated for the sampling sites including several metagenomes. Air sites (*i.e.* our 9 sites + 5
 252 sites where public air metagenomes come from) are distinguished by grey hatching lines.

253

254

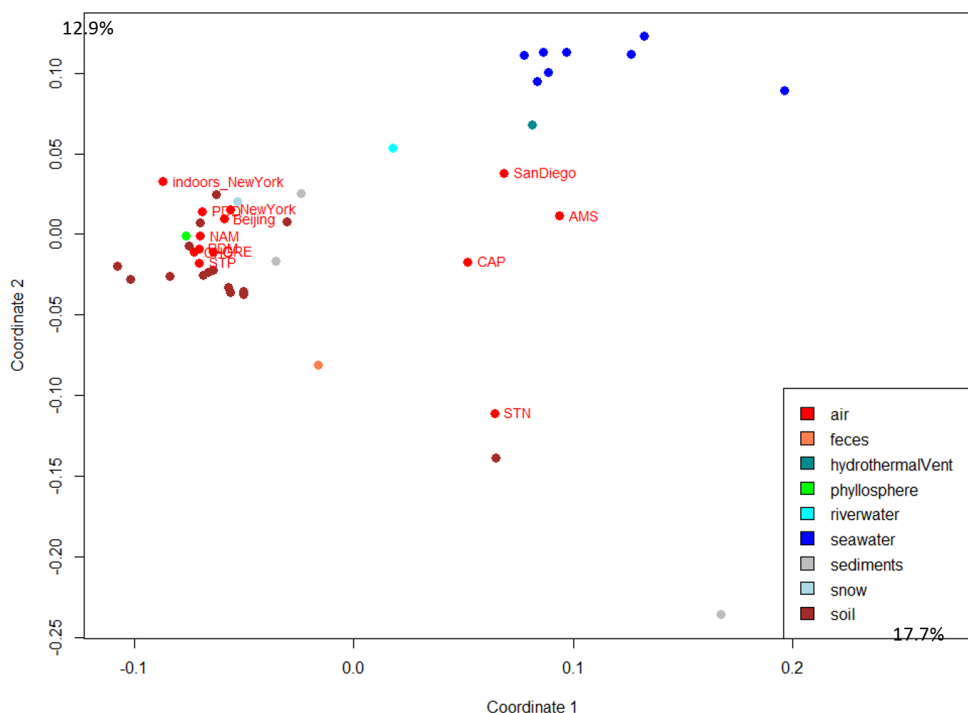
255 3.2 Airborne microbial functional profiles

256

257 The fifty most abundant SEED functional classes represented in atmospheric samples are listed
 258 in **Table S5**. The 5-FCL-like protein, the long chain fatty acid CoA ligase and the TonB-
 259 dependent receptor were the top three functions based on number of annotated reads observed
 when including all the sequences (**Table S5**). The atmospheric microbial functional profiles



260 based on the SEED functions were compared between samples from the different weeks of
261 sampling and between different locations. The profiles were graphed using PCo multivariate
262 analysis to visualize differences and similarities. The different samples (sampled during
263 sequential weeks) from the same site did not cluster tightly together on the PCo multivariate
264 analysis. In order to incorporate weekly variation when comparing sites, we used the microbial
265 functional profile averaged per site in the subsequent multivariate analyses done with the data
266 from other ecosystems (**Fig 3**). The PCo multivariate analysis showed that terrestrial
267 atmospheric sites (GRE, NAM, STP, PDD, PDM, CHC, New York) grouped with the soil,
268 sediment and snow samples while the marine and coastal atmospheric sites (AMS, CAP, San
269 Diego) were situated between the datasets from soil, seawater and river water (**Fig 3**). The polar
270 site STN did not group with the other sites. When considering only the bacterial sequences (*i.e.*,
271 excluding the fungal sequences), the distribution of the terrestrial atmospheric sites did not
272 change, while the marine Amsterdam-Island, coastal Cape Point and polar Station Nord
273 atmospheric sites were further from the seawater and river water datasets than when the fungal
274 sequences were included (**Fig S2**). The distribution of the different datasets underwent further
275 changes when considering only the fungal sequences. We observed an absence of a clear
276 separation between soil and seawater since they (for the majority) grouped closely together, and
277 terrestrial atmospheric datasets did not group with the other non-atmospheric datasets from soil,
278 sediment and snow (**Fig S2**).
279



280
281 **Fig 3. Distribution of the samples based on the microbial functional profile.** The PCo
282 analysis of the Bray-Curtis dissimilarity matrix is based on the functional potential structure of
283 each site. For the site including several metagenomes, the average profile was calculated. Colors
284 indicate the ecosystems in which the sites belong to.



285

286

3.3 Airborne microbial functional richness and evenness

287

Functional richness and evenness were evaluated using the relative abundance of sequences in the different SEED categories. The average richness in SEED functional classes (or functions) in the PBL was lower than the average functional class richness in soil, surface seawater, hydrothermal vents, river water, phyllosphere and feces ($P < 0.05$) (Table S3). Among the different atmospheric samples, the functional class richness was highest in Beijing (4060 +/- 112 functional classes) and New York indoor air samples (3302 +/- 299 functional classes) ($P < 0.05$), and lowest in Station Nord (956 +/- 547 functional classes). When looking at the bacteria-annotated sequences, almost the same trend was observed, *i.e.* the functional class richness in air was lower than in soil, hydrothermal vents, river water, phyllosphere and feces, and not different from the other ecosystems ($P < 0.05$ and > 0.05 , respectively) (Table S3). The functional class richness was higher in Beijing (2835 +/- 59 functional classes) and New York indoor air samples (2183 +/- 387 functional classes) compared to the other air samples whose values ranged between 270 +/- 197 functional classes in Amsterdam-Island and 1142 +/- 461 functional classes in Chacaltaya. For fungal sequences, the functional class richness in the atmosphere was lower than the functional class richness in soil, surface seawater, feces, hydrothermal vents, river water and phyllosphere ($P < 0.05$) (Table S3). Within air samples, the functional class richness based on fungal sequences was higher in Beijing (1129 +/- 92 functional classes) and New York indoor air samples (687 +/- 206 functional classes) than in the other air sites ($P < 10^{-5}$) whose values ranged from 66 +/- 58 functional classes in Amsterdam-Island and 392 +/- 131 functional classes in Storm Peak (Table S3). The functional class evenness in air was on average higher than in soil ($P = 0.03$), and not different to the functional class evenness observed in the other ecosystems (sediment, seawater, snow). When looking at the bacterial and fungal sequences separately, the functional class evenness in air was on average higher than in soil, feces, phyllosphere and riverwater ($P < 0.05$) (Table S3).

311

312

3.4 Concentration of specific microbial functions that might have a role under atmospheric conditions

313

314

Two metabolic functions associated with abundant atmospheric chemicals (H_2O_2 and CH_4) were examined, hydrogen catabolism and methane monooxygenase activity. The concentration of sequences annotated as hydrogen peroxide catabolic related functional proteins per 10000 sequences varied between air sites ($P = 2 \times 10^{-5}$) with highest values for Amsterdam-Island (27 +/- 1) and Grenoble (27 +/- 1) (Fig S3). It was on average higher in air compared to soil ($P = 10^{-4}$) and surface seawater ($P = 10^{-4}$). The French agricultural soil showed the highest relative abundance (133 +/- 4). When considering the fungal and bacterial sequences separately, this concentration was not different between air and the other ecosystems ($P > 0.05$) (Fig S3). The number of sequences annotated as methane monooxygenase-related functional proteins per 10000 sequences was only detectable when considering all the sequences (*i.e.* bacterial and fungal sequences). The number of sequences annotated as methane monooxygenase-related functional proteins did not vary between air sites ($P > 0.05$) while we observed a high variability between sampling periods within sites, but on average it was not different from the ecosystems ($P > 0.05$).

328

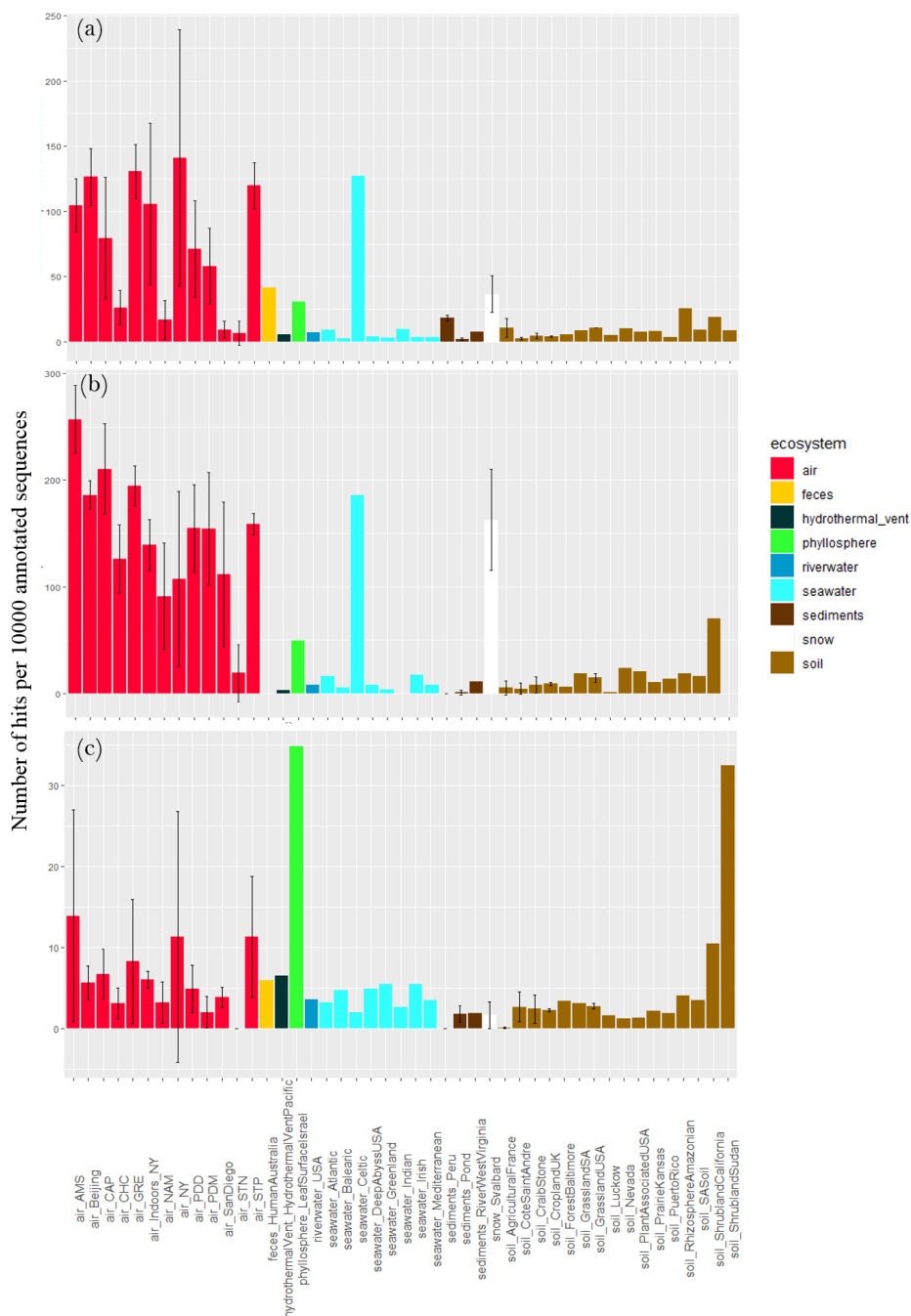
329

Different stress response functions (sporulation, UV response, oxidative stress cell response, desiccation response, chromosome plasmid partitioning protein ParA and lipoate synthase) were examined. The concentration of sequences annotated as sporulation-related functional proteins per 10000 annotated sequences largely varied between air sites ($P = 2 \times 10^{-9}$), with the lowest values observed for Station Nord (7 +/- 9), San Diego (9 +/- 6), Namco (17 +/- 15) and Chacaltaya (26 +/- 13), and the highest values observed for Storm Peak (120 +/- 18), Beijing (126 +/- 22), Grenoble (131 +/- 21) and New York (141 +/- 98) (Fig 4). It was on average higher

334



335 in air compared to soil ($P < 10^{-5}$), sediments ($P < 10^{-5}$) and surface seawater ($P = 4 \times 10^{-4}$) although
336 the Celtic seawater sample presented a very high concentration (127). Snow showed a relatively
337 high average concentration (*i.e.* 36) which was not different from air concentration ($P > 0.05$).
338 For the ecosystems including one value (*i.e.* one sample, so not integrated in the Kruskal-Wallis
339 tests), feces showed a relatively high concentration of sequences annotated as sporulation-
340 related functional proteins (*i.e.* 41) while hydrothermal vent, phyllosphere and river water
341 showed relatively low concentrations compared to air (< 10). When considering the fungal
342 sequences separately from the bacterial sequences, the same trend was observed, *i.e.* the
343 concentration of sequences annotated as sporulation-related functional proteins in air was on
344 average higher compared to soil ($P < 10^{-5}$), sediments ($P < 10^{-5}$), surface seawater ($P = 7 \times 10^{-4}$) as
345 well as phyllosphere, hydrothermal vent and river water. The concentration was relatively high
346 in the Celtic seawater (186) and the snow samples (163 +/- 47). We also observed a large
347 variability within air sites ($P = 3 \times 10^{-5}$). When considering the bacterial sequences only, this
348 concentration in air was on average higher compared to soil ($P = 0.02$), sediments ($P = 4 \times 10^{-3}$)
349 and snow ($P = 0.01$), and showed a smaller variability between air sites. Two samples, the
350 phyllosphere (*i.e.* 35) and the shrubland soil from Sudan (*i.e.* 32) showed high numbers of
351 sequences annotated as sporulation-related functional proteins per 10000 annotated sequences
352 (**Fig 4**).
353



354

355

356

357

Fig 4. Proportion of sequences annotated as sporulation related functional proteins in the metagenomes. Average number of sequences annotated as proteins implicated in sporulation per 10000 annotated sequences from (a) all sequences, (b) fungal sequences and (c) bacterial



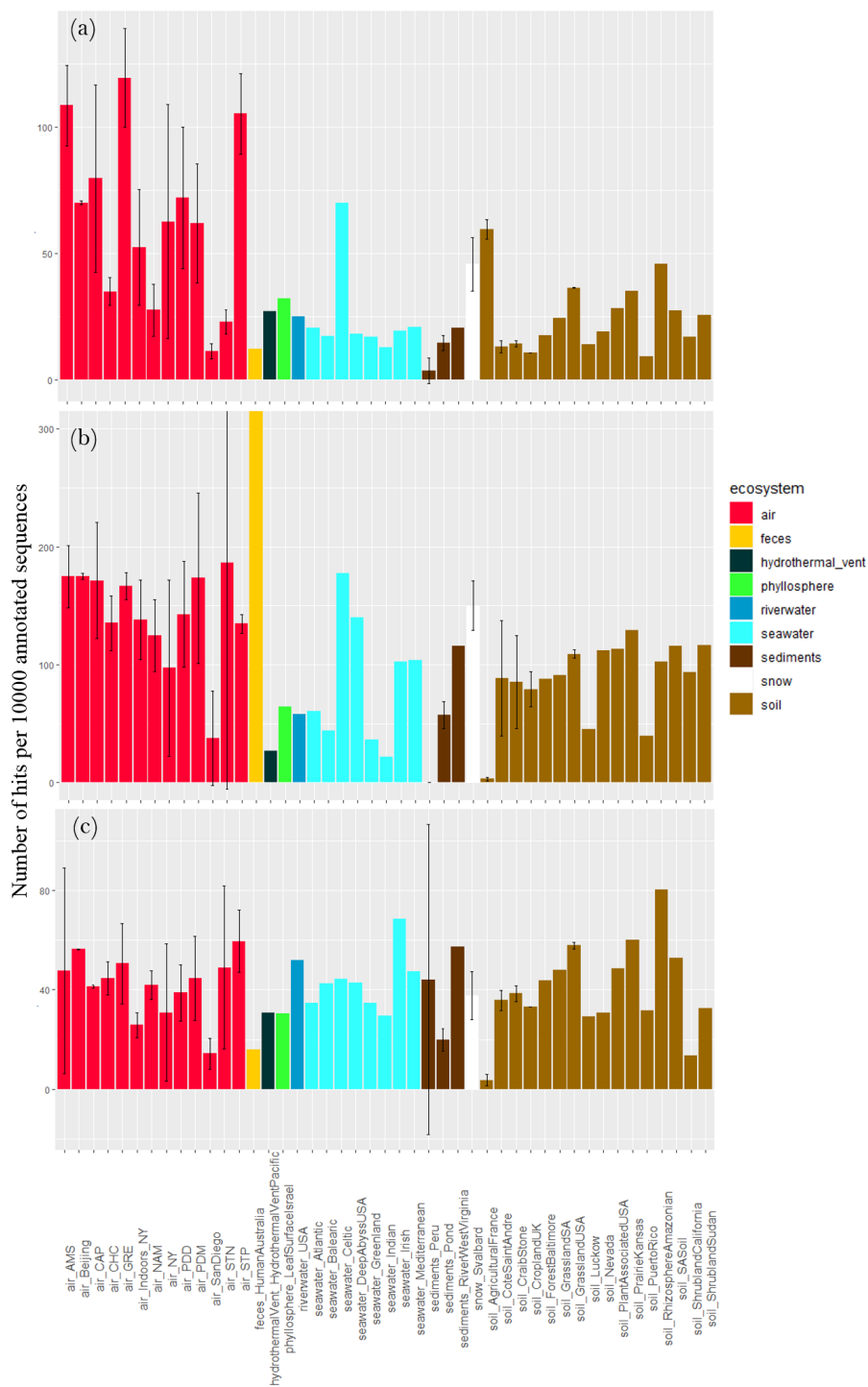
358 sequences per site. Colors indicate the ecosystems in which the sites belong to. For the sites
359 including several metagenomes, the standard deviation was added.

360

361 The concentration of sequences annotated as UV response related functional proteins per 10000
362 annotated sequences varied between air sites ($P=10^{-5}$), with values ranging from 16 +/- 2 in
363 Namco and 19 +/- 4 in STN to 29 +/- 3 in Storm Peak and 36 +/- 6 in Amsterdam-Island (**Fig**
364 **S4**). The concentration was on average higher in air compared to sediments ($P<10^{-5}$), soil
365 ($P<10^{-5}$) and comparable to snow and surface seawater ($P>0.05$). The other ecosystems showed
366 lower ratios (feces, phyllosphere) or comparable concentrations (hydrothermal vent, river
367 water) compared to air. Within the soil samples, the French agricultural soil samples showed a
368 high average concentration (56 +/- 8), which increased the average ratio observed in soil
369 samples. When considering fungal sequences separately, the concentration of sequences
370 annotated as UV response related functional proteins was higher in air compared to soil
371 ($P=9\times 10^{-4}$), and comparable to the other ecosystems ($P>0.05$). When considering the bacterial
372 sequences only, this concentration in air was on average higher compared to seawater ($P=3\times 10^{-3}$)
373 and sediments ($P=6\times 10^{-3}$).

374 The concentration of sequences annotated as oxidative stress cell response related functional
375 proteins per 10000 annotated sequences varied largely between air sites ($P=5\times 10^{-7}$), with the
376 lowest values observed for Station Nord (23 +/- 5), San Diego (11 +/- 3) and Namco (28 +/-
377 10), and the highest values observed for Storm Peak (105 +/- 16), Amsterdam-Island (108 +/-
378 16) and Grenoble (119 +/- 19) (**Fig 5**). The concentration was on average higher in air compared
379 to soil ($P<10^{-5}$), sediments ($P<10^{-5}$) and surface seawater ($P=2\times 10^{-3}$). Snow showed a relatively
380 high average value (46 +/- 11), not different from air ($P>0.05$). The other ecosystems (feces,
381 river water, hydrothermal vent, phyllosphere) showed lower ratios compared to air. When
382 considering fungal sequences separately, the concentration of sequences annotated as oxidative
383 stress related functional proteins per 10000 sequences was on average higher in air compared
384 to soil ($P<10^{-5}$), sediments ($P<10^{-5}$) and surface seawater ($P=10^{-3}$). Feces showed a very high
385 average value (2237). When considering bacterial sequences separately, this concentration was
386 not different between air and the other ecosystems ($P>0.05$). When considering both fungal and
387 bacterial sequences separately, the variability in the concentration of sequences annotated as
388 oxidative stress cell response related functional proteins between air sites diminished and their
389 difference was not detected anymore ($P>0.05$).

390





392 **Fig 5. Proportion of sequences as oxidative stress cell response related functional proteins**
393 **in the metagenomes.** Average number of sequences annotated as proteins implicated in
394 oxidative stress cell response per 10000 annotated sequences from (a) all sequences, (b) fungal
395 sequences and (c) bacterial sequences per site. Colors indicate the ecosystems in which the sites
396 belong to. For the sites including several metagenomes, the standard deviation was added.

397
398

399 The concentration of sequences annotated as desiccation response related functional proteins
400 per 10000 sequences varied between air sites ($P=2\times 10^{-5}$), with the highest values in Grenoble
401 (4 +/- 1), Storm Peak (4 +/- 1) and Amsterdam-Island (3 +/- 3), and the lowest values in Station
402 Nord (0.5 +/- 1) and San Diego (0.1 +/- 0.1) (Fig S4). It was on average higher in air compared
403 to the other ecosystems ($P=4\times 10^{-9}$). Still Svalbard snow and French agricultural soil showed
404 high values (2 +/- 1 and 3 +/- 1, respectively) (Fig S4). When considering fungal sequences
405 only, the concentration in air was higher compared to soil ($P>10^{-5}$), sediments ($P>10^{-5}$) and
406 surface seawater ($P=10^{-3}$). No difference between the ecosystems was observed when
407 considering bacterial sequences separately ($P=0.62$).

408 Two proteins (lipoate synthase and chromosome plasmid partitioning protein ParA) related to
409 stress response showed high relative concentrations in bacterial sequences of a few air samples
410 compared to the other ecosystems (Fig S3), although the number of sequences related to these
411 proteins was on average not higher in the atmosphere than other ecosystems ($P>0.05$).

412

413 4 Discussion

414 Metagenomic investigations of different ecosystems revealed a specific functional potential
415 signature of their associated microbial communities (Delmont et al., 2011; Tringe et al., 2005).
416 These specific signatures are thought to result from microbial adaptation and/or physical
417 selection to the environmental abiotic conditions (Hindré et al., 2012; Li et al., 2019; Rey et al.,
418 2016) and are a reflection of the high relative abundances of genes coding for specific functions
419 essential for microorganisms to survive and develop in these environments. For example,
420 microbial metagenomes of human feces were characterized by high relative abundances of
421 sequences annotated as beta-glucosidases that are associated with high intestinal concentrations
422 of complex glycosides; and microbial metagenomes of oceans were enriched in sequences
423 annotated as enzymes catalyzing DMSP (dimethylsulfoniopropionate), that is an organosulfur
424 compound produced by phytoplankton (Delmont et al., 2011). Our results showed a clear
425 separation between surface seawater, river water, human feces and almost all the soil samples
426 (which grouped with the sediment and snow samples at the scale used here) on the PCo analysis
427 based on the microbial functional potential (Fig 3). For air microbiomes, the PCo analyses
428 showed that the individual air samples did not group for each site and that they did not form a
429 cluster separated from the other ecosystems based on the overall microbial functional potential
430 averaged per site (Fig 3). Air samples seemed to group with their underlying ecosystems. While
431 terrestrial air samples (GRE, NAM, CHC, STP, PDD, PDM) grouped with snow, soil and
432 sediment samples, the marine (Amsterdam-Island), coastal (Cape Point) and arctic (Station
433 Nord) air samples were closer to surface seawater and river water samples. Airborne microbial
434 functional potential (and especially metabolic functional potential as SEED functional classes
435 included mainly metabolic functions and few stress response related functions) might be
436 dependent on the ecosystems from which microorganisms are aerosolized. Moreover, it seems
437 that bacterial sequences are mainly responsible for the distribution of the samples on the PCo
438 analysis (as observed when comparing the PCoA to that carried out with the fungal sequences
439 only) although they were in smaller numbers compared to fungal sequences for many of the air
440 samples (*i.e.* STP, GRE, AMS, PDD, CAP, Beijing *etc.*). The low statistical weight of fungal
441 sequences relative to the overall sequences might be related to their low richness in terms of

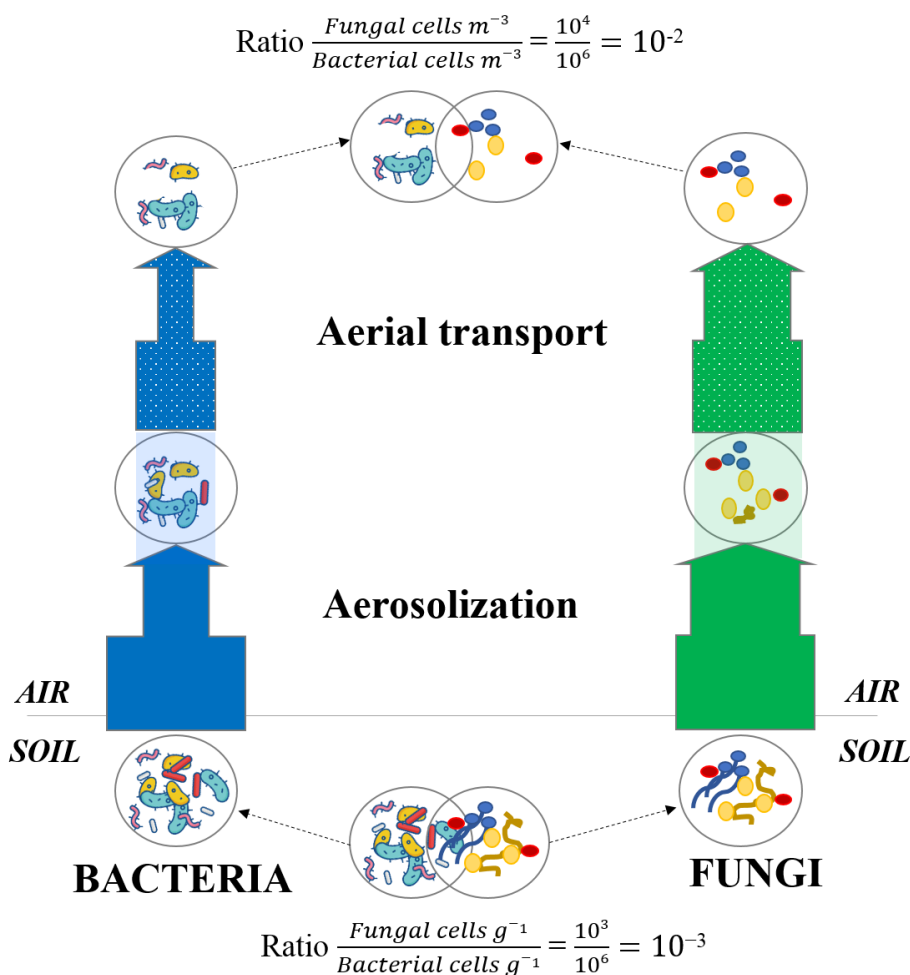


442 functional genes that might have resulted in the spreading of the samples on the PCoA based
443 on the fungal sequences (**Table S3**).

444 Metagenomes extracted from atmospheric samples taken around the planet were characterized
445 by a relatively high percentage of fungal sequences as compared to other ecosystems even
446 though bacterial sequences still dominated. This percentage varied across the different sites
447 with a higher percentage at terrestrial sites whose surrounding landscapes were vegetated like
448 Grenoble (GRE), puy de Dôme (PDD) and Pic-du-midi (PDM) (surrounding landscapes in **Fig**
449 **S1**). This percentage was also relatively high at the marine site Amsterdam-Island (AMS),
450 where fungi might come from the ocean and/or the vegetated surfaces of the small island. A
451 high percentage of fungal sequences was also reported for air samples from Beijing, New York
452 and San Diego and validates our DNA extraction method set-up specifically for quartz fiber
453 filter (Dommergue et al., 2019). Similarly, the sequencing technology (Illumina MiSeq) could
454 not have been responsible for the larger percentage of fungal sequences observed in our datasets
455 as the Beijing and New York/San Diego air sample datasets originated from Illumina HiSeq
456 and 454 sequencing technology, respectively. qPCR results on the 16S rRNA gene (bacterial
457 cell concentration estimation) and on the 18S rRNA gene (fungal cell concentration estimation)
458 on our air samples in comparison to soil samples (Côte Saint André, France) showed that the
459 ratio between fungal and bacterial cell number was much higher (from 4.5 to 160 times higher
460 for the most vegetated site Grenoble) in air than in soil (**Table S4**). The ratio between fungal
461 and bacterial cell number might be higher in the planetary boundary layer (PBL) than in other
462 environments like soil (Malik et al., 2016), and thus, would explain the relatively higher
463 percentage of fungal sequences observed in air metagenomes. High throughput sequencing
464 allows the sequencing of a small part of the metagenomic DNA (with large fungal genomes
465 likely to be sequenced first) and might explain why the values of the bacteria and fungi
466 abundance ratio obtained by qPCR does not match those obtained by the metagenomic
467 sequencing approach. Our study is a preliminary metagenomic investigation of the air
468 environment with a limited number of sequences per sample, and further studies are needed to
469 confirm our results.

470 Fungi in the atmosphere are expected to be found mostly as fungal spores, although the relative
471 concentration of fungal spores and fungal hyphae fragments in air is unknown. Our results
472 showed that the number of sporulation-related functions was higher in air than the other
473 ecosystems (with the exception of snow and phyllosphere). While fungal hyphae are not
474 expected to be particularly resistant to extreme conditions such as UV radiation, fungal spores
475 are specifically produced to resist and survive overall adverse atmospheric conditions (Huang
476 and Hull, 2017). Their thick membrane and dehydrated nature make them particularly resistant
477 to abiotic atmospheric conditions such as UV radiation, oxidative stress, desiccation as well as
478 osmotic stress. **Fig 6** presents a conceptual model that could explain the higher ratio between
479 fungi and bacteria observed in air. During aerosolization and aerial transport, bacteria and fungi
480 might be under stress and might undergo a physical selection with the survival of the most
481 resistant cells to the adverse atmospheric conditions (*i.e.* UV radiation, desiccation *etc.*) and the
482 death of non-resistant cells. As fungi (and especially fungal spores) might be naturally more
483 resistant and adapted to atmospheric conditions than bacteria, we expect a larger decline of
484 bacterial cells compared to fungal cells and spores in air. This might have as a consequence an
485 increase in the ratio between fungi and bacteria compared to their non-atmospheric origins (*i.e.*
486 the surrounding ecosystems) (**Fig 6**).

487



488
 489
 490
 491
 492
 493
 494
 495
 496
 497

Fig 6. Microbial cell loss due to atmospheric physical stress. Conceptual model on the microbial cell loss occurring during the aerosolization and aerial transport steps due to physical selection. The thickness of the arrows represents the impact of the physical selection on both bacterial and fungal cell loss (the more microbial cells survive the physical selection, the thicker becomes the arrow). Approximate ratios are indicative and result from 16S rRNA and 18S rRNA qPCR data on Côte Saint André soil samples (crop soil, France) and puy de Dôme air samples (France; puy de Dôme landscape is mainly composed of croplands as shown in Fig S1).

498
 499
 500
 501
 502
 503

The high variability between the air sites and between air samples of the same site could be explained by the variability in the inputs from the different surrounding landscapes. Our previous paper showed that local inputs were the main sources of planetary boundary layer microorganisms and that local meteorology (especially the wind direction) had a major impact on the temporal variability of airborne microbial communities by affecting which of the



504 different local sources were upwind (Tignat-Perrier et al., 2019). Our results did not show a
505 specific (metabolic) functional potential signature for the atmosphere, which was rather mainly
506 driven by the surrounding landscapes. Our results are consistent with both a pre-metabolic
507 adaptation of airborne microorganisms to the chemicals of the sources (*i.e.* surrounding
508 landscapes) and a potential metabolic adaptation to these chemicals in the atmosphere.
509 Atmospheric chemistry is dependent on the underlying ecosystem chemistry since the main
510 sources of atmospheric chemicals are Earth surface emissions. Yet, the oxidizing conditions of
511 the atmosphere might lead to rapid transformations of atmospheric chemicals by photochemical
512 reactions. These specific atmospheric chemical reactions (*i.e.* photochemical) produce species
513 which, with the gases like CH₄, characterize the atmosphere (O₃, H₂O₂, OH *etc.*). Although
514 some microbial strains from cloud water origin have been shown to metabolize and grow on
515 culture medium in the presence of H₂O₂ (Vařtilingom et al., 2013), radical species and their
516 precursors are reactive compounds and might not easily serve as energy and carbon sources for
517 microorganisms (Imlay, 2013). Our results on specific metabolic related functions showed that
518 functions related to methane monooxygenase activity (CH₄ degradation) and hydrogen
519 peroxide catabolism (H₂O₂ degradation) were present in air but not in higher proportion than in
520 other ecosystems (**Fig S3**). Reactive compounds can cause oxidative stress to airborne
521 microorganisms. In association to adverse physical conditions like UV radiation and
522 desiccation, oxidative compounds might create more of a physical stress than provide a new
523 metabolic source for airborne microorganisms. Laboratory investigations of cultivable
524 microorganisms of an airborne origin showed the presence of particularly resistant strains under
525 stressful conditions similar to the atmospheric ones (*i.e.* similar UV radiation levels; different
526 oxidative conditions) (Joly et al., 2015; Yang et al., 2008). However, no study has shown
527 whether these apparently adapted cells represented the majority of airborne microorganisms.
528 Since the overall SEED functional classes included mainly metabolic functions, specific stress
529 related functions using GO (Gene Ontology) terms were also evaluated. We observed that on
530 average, air showed more stress-related functions (UV response, desiccation and oxidative
531 stress response related functions) than the other ecosystems due to the higher concentration of
532 fungi (relatively to bacteria) in air. Thus, when the annotated sequences were separated between
533 sequences belonging to fungal and bacterial genomes, the bacterial and fungal sequences from
534 air samples did not show a significantly higher concentration of stress-related functions
535 compared to the samples coming from other ecosystems (**Fig 4, 5, Fig S4**).
536 Fungal genomes are expected to carry genes associated to global stress-related functions (*i.e.*
537 UV radiation, desiccation, oxidative stress), because of the innate resistance of fungi especially
538 fungal spores. These genes associated to global stress-related functions are likely acquired
539 during sporulation formation and certainly do not result from adaptation of fungi in air. When
540 studying genes coding more specific proteins that are not associated to spore resistance, such
541 as lipoate synthase and chromosome plasmid partitioning protein ParA, that might play a role
542 in oxidative stress (Allary et al., 2007; Bunik, 2003) and are more generally found in stress
543 resistance and adaptability of microorganisms (Shoeb et al., 2012; Zhang et al., 2018), they
544 were occasionally found in relatively high concentration in air samples (**Fig S3**). The detection
545 of metagenomic sequences annotated as genes coding specific proteins in air samples remains
546 difficult because of the low microbial biomass recovered. That is why we examined the
547 presence and concentration of global functions (*i.e.* UV protection related functions, oxidative
548 stress response related functions *etc.*) rather than specific functional genes.
549 The constant and large input of microbial cells to the planetary boundary layer and their
550 relatively short residence time (a few hours to a few days based on a model assuming that
551 microbial cells behave like non biological aerosols (Jaenicke, 1980)) might have hindered the
552 observation of the potential adaptation (physical selection and/or microbial adaptation) of
553 airborne microorganisms to the stressful atmospheric conditions and to the atmospheric



554 chemicals as discussed above. This issue might be addressed by investigating microbial
555 functional potential in the free troposphere (preferentially high enough above the ground so as
556 not to be influenced by the surface) where the microbial fluxes are smaller than in the planetary
557 boundary layer and where microbial airborne residence time might last much longer than in the
558 planetary boundary layer. This troposphere approach might help in determining the role of
559 stress in the atmosphere and validate our conceptual model on the physical stress of microbial
560 cells taking place during aerosolization and aerial transport selecting the resistant cells (**Fig 6**).
561 Another explanation might be due to the metagenomic approach that allows to sample both
562 living and dead cells. Aerosolization has been shown to be particularly stressful and even lethal
563 for microorganisms (Alsved et al., 2018; Thomas et al., 2011). The functional potential from
564 the dead cells in air might have a greater weight on the overall functional potential observed
565 and lead to the dilution of the functional potential of the actual living cells that have adapted to
566 atmospheric conditions. This might apply for both the overall functional potential discussed
567 previously and the stress-related functions.

568

569 **Conclusion**

570 We conducted the first global comparative metagenomic analysis to characterize the microbial
571 functional potential signature in the planetary boundary layer. Air samples showed no specific
572 signature of microbial functional potential which was mainly correlated to the surrounding
573 landscapes. However, air samples were characterized by a relatively high percentage of fungal
574 sequences compared to the source ecosystems (soil, surface seawater *etc.*). The relatively higher
575 concentrations of fungi in air drove the higher proportions of stress-related functions observed
576 in air metagenomes. Fungal cells and specifically fungal spores are innately resistant entities
577 well adapted to atmospheric conditions and which might survive better aerosolization and aerial
578 transport than bacterial cells. Stress-related functions were present in airborne bacteria but
579 rarely in higher concentrations compared to the bacterial communities in other ecosystems.
580 However, the constant flux of microbial cells to the planetary boundary layer might have
581 complicated the determination of a physical selection and/or microbial adaptation of airborne
582 microorganisms, especially bacterial communities. Meta-omics investigations on air with a
583 deeper sequencing are needed to confirm our results and explore the functionality of
584 atmospheric microorganisms further.

585

586 **References**

- 587 Aalismail, N. A., Ngugi, D. K., Díaz-Rúa, R., Alam, I., Cusack, M. and Duarte, C. M.: Functional
588 metagenomic analysis of dust-associated microbiomes above the Red Sea, *Sci Rep*, 9(1), 1–12,
589 doi:10.1038/s41598-019-50194-0, 2019.
- 590 Allary, M., Lu, J. Z., Zhu, L. and Prigge, S. T.: Scavenging of the cofactor lipoate is essential for the
591 survival of the malaria parasite *Plasmodium falciparum*, *Mol Microbiol*, 63(5), 1331–1344,
592 doi:10.1111/j.1365-2958.2007.05592.x, 2007.
- 593 Alsved, M., Holm, S., Christiansen, S., Smidt, M., Ling, M., Boesen, T., Finster, K., Bilde, M.,
594 Löndahl, J. and Šantl-Temkiv, T.: Effect of Aerosolization and Drying on the Viability of
595 *Pseudomonas syringae* Cells, *Front Microbiol*, 9, 3086, doi:10.3389/fmicb.2018.03086, 2018.
- 596 Amato, P., Demeer, F., Melaouhi, A., Fontanella, S., Martin-Biesse, A.-S., Sancelme, M., Laj, P. and
597 Delort, A.-M.: A fate for organic acids, formaldehyde and methanol in cloud water: their
598 biotransformation by micro-organisms, *Atmospheric Chemistry and Physics*, 7(15), 4159–4169,
599 doi:https://doi.org/10.5194/acp-7-4159-2007, 2007.
- 600 Amato, P., Besaury, L., Joly, M., Penaud, B., Deguillaume, L. and Delort, A.-M.: Metatranscriptomic
601 exploration of microbial functioning in clouds, *Sci Rep*, 9(1), 1–12, doi:10.1038/s41598-019-41032-4,
602 2019.



- 603 Ariya, P., Sun, J., Eltouny, N., Hudson, E., Hayes, C. and Kos, G.: Physical and chemical
604 characterization of bioaerosols—Implications for nucleation processes, *International Reviews in*
605 *Physical Chemistry*, 28, 1–32, doi:10.1080/01442350802597438, 2009.
- 606 Ariya, P. A., Nepotchatykh, O., Ignatova, O. and Amyot, M.: Microbiological degradation of
607 atmospheric organic compounds, *Geophysical Research Letters*, 29(22), 34–1–34–4,
608 doi:10.1029/2002GL015637, 2002.
- 609 Aylor, D. E.: Spread of Plant Disease on a Continental Scale: Role of Aerial Dispersal of Pathogens,
610 *Ecology*, 84(8), 1989–1997, 2003.
- 611 Brown, J. K. M. and Hovmöller, M. S.: Aerial dispersal of pathogens on the global and continental
612 scales and its impact on plant disease, *Science*, 297(5581), 537–541, doi:10.1126/science.1072678,
613 2002.
- 614 Brune, A., Frenzel, P. and Cypionka, H.: Life at the oxic–anoxic interface: microbial activities and
615 adaptations, *FEMS Microbiol Rev*, 24(5), 691–710, doi:10.1111/j.1574-6976.2000.tb00567.x, 2000.
- 616 Bunik, V. I.: 2-Oxo acid dehydrogenase complexes in redox regulation, *Eur. J. Biochem.*, 270(6),
617 1036–1042, doi:10.1046/j.1432-1033.2003.03470.x, 2003.
- 618 Cao, C., Jiang, W., Wang, B., Fang, J., Lang, J., Tian, G., Jiang, J. and Zhu, T. F.: Inhalable
619 Microorganisms in Beijing’s PM_{2.5} and PM₁₀ Pollutants during a Severe Smog Event, *Environ. Sci.*
620 *Technol.*, 48(3), 1499–1507, doi:10.1021/es4048472, 2014.
- 621 Chemidlin Prévost-Bouré, N., Christen, R., Dequiedt, S., Mougél, C., Lelièvre, M., Jolivet, C.,
622 Shahbazkia, H. R., Guillou, L., Arrouays, D. and Ranjard, L.: Validation and application of a PCR
623 primer set to quantify fungal communities in the soil environment by real-time quantitative PCR,
624 *PLoS ONE*, 6(9), e24166, doi:10.1371/journal.pone.0024166, 2011.
- 625 Delmont, T. O., Malandain, C., Prestat, E., Larose, C., Monier, J.-M., Simonet, P. and Vogel, T. M.:
626 Metagenomic mining for microbiologists, *ISME J*, 5(12), 1837–1843, doi:10.1038/ismej.2011.61,
627 2011.
- 628 Delort, A.-M., Vaïtilingom, M., Amato, P., Sancelme, M., Parazols, M., Mailhot, G., Laj, P. and
629 Deguillaume, L.: A short overview of the microbial population in clouds: Potential roles in
630 atmospheric chemistry and nucleation processes, *Atmospheric Research*, 98(2), 249–260,
631 doi:10.1016/j.atmosres.2010.07.004, 2010.
- 632 Dommergue, A., Amato, P., Tignat-Perrier, R., Magand, O., Thollot, A., Joly, M., Bouvier, L.,
633 Sellegri, K., Vogel, T., Sonke, J. E., Jaffrezo, J.-L., Andrade, M., Moreno, I., Labuschagne, C., Martin,
634 L., Zhang, Q. and Larose, C.: Methods to investigate the global atmospheric microbiome, *Front.*
635 *Microbiol.*, 10, doi:10.3389/fmicb.2019.00243, 2019.
- 636 Donovan, P. D., Gonzalez, G., Higgins, D. G., Butler, G. and Ito, K.: Identification of fungi in
637 shotgun metagenomics datasets, *PLOS ONE*, 13(2), e0192898, doi:10.1371/journal.pone.0192898,
638 2018.
- 639 Els, N., Larose, C., Baumann-Stanzer, K., Tignat-Perrier, R., Keuschnig, C., Vogel, T. M. and Sattler,
640 B.: Microbial composition in seasonal time series of free tropospheric air and precipitation reveals
641 community separation, *Aerobiologia*, doi:10.1007/s10453-019-09606-x, 2019.
- 642 Fierer, N., Jackson, J. A., Vilgalys, R. and Jackson, R. B.: Assessment of Soil Microbial Community
643 Structure by Use of Taxon-Specific Quantitative PCR Assays, *Appl. Environ. Microbiol.*, 71(7),
644 4117–4120, doi:10.1128/AEM.71.7.4117-4120.2005, 2005.



- 645 Friedl, M. A., McIver, D. K., Hodges, J. C. F., Zhang, X. Y., Muchoney, D., Strahler, A. H.,
646 Woodcock, C. E., Gopal, S., Schneider, A., Cooper, A., Baccini, A., Gao, F. and Schaaf, C.: Global land
647 cover mapping from MODIS: algorithms and early results, *Remote Sensing of Environment*, 83(1),
648 287–302, doi:10.1016/S0034-4257(02)00078-0, 2002.
- 649 Griffin, D. W.: Atmospheric Movement of Microorganisms in Clouds of Desert Dust and
650 Implications for Human Health, *Clin Microbiol Rev*, 20(3), 459–477, doi:10.1128/CMR.00039-06,
651 2007.
- 652 Gusareva, E. S., Acerbi, E., Lau, K. J. X., Luhung, I., Premkrishnan, B. N. V., Kolundžija, S.,
653 Purbojati, R. W., Wong, A., Houghton, J. N. I., Miller, D., Gaultier, N. E., Heinle, C. E., Clare, M. E.,
654 Vettath, V. K., Kee, C., Lim, S. B. Y., Chénard, C., Phung, W. J., Kushwaha, K. K., Nee, A. P., Putra,
655 A., Panicker, D., Yanqing, K., Hwee, Y. Z., Lohar, S. R., Kuwata, M., Kim, H. L., Yang, L., Uchida, A.,
656 Drautz-Moses, D. I., Junqueira, A. C. M. and Schuster, S. C.: Microbial communities in the tropical
657 air ecosystem follow a precise diel cycle, *PNAS*, 116(46), 23299–23308,
658 doi:10.1073/pnas.1908493116, 2019.
- 659 Hadley, W. and Winston, C.: Create Elegant Data Visualisations Using the Grammar of Graphics,
660 [online] Available from: <https://cran.r-project.org/web/packages/ggplot2/ggplot2.pdf>, 2019.
- 661 Hill, K. A., Shepson, P. B., Galbavy, E. S., Anastasio, C., Kourtev, P. S., Konopka, A. and Stirm, B. H.:
662 Processing of atmospheric nitrogen by clouds above a forest environment, *Journal of Geophysical*
663 *Research: Atmospheres*, 112(D11), doi:10.1029/2006JD008002, 2007.
- 664 Hindré, T., Knibbe, C., Beslon, G. and Schneider, D.: New insights into bacterial adaptation through
665 *in vivo* and *in silico* experimental evolution, *Nature Reviews Microbiology*, 10(5), 352–365,
666 doi:10.1038/nrmicro2750, 2012.
- 667 Huang, M. and Hull, C. M.: Sporulation: How to survive on planet Earth (and beyond), *Curr Genet*,
668 63(5), 831–838, doi:10.1007/s00294-017-0694-7, 2017.
- 669 Huerta-Cepas, J., Forslund, K., Coelho, L. P., Szklarczyk, D., Jensen, L. J., von Mering, C. and Bork,
670 P.: Fast Genome-Wide Functional Annotation through Orthology Assignment by eggNOG-Mapper,
671 *Mol. Biol. Evol.*, 34(8), 2115–2122, doi:10.1093/molbev/msx148, 2017.
- 672 Huson, D. H., Richter, D. C., Mitra, S., Auch, A. F. and Schuster, S. C.: Methods for comparative
673 metagenomics, *BMC Bioinformatics*, 10 Suppl 1, S12, doi:10.1186/1471-2105-10-S1-S12, 2009.
- 674 Imlay, J. A.: The molecular mechanisms and physiological consequences of oxidative stress: lessons
675 from a model bacterium, *Nat Rev Microbiol*, 11(7), 443–454, doi:10.1038/nrmicro3032, 2013.
- 676 Innocente, E., Squizzato, S., Visin, F., Facca, C., Rampazzo, G., Bertolini, V., Gandolfi, I., Franzetti,
677 A., Ambrosini, R. and Bestetti, G.: Influence of seasonality, air mass origin and particulate matter
678 chemical composition on airborne bacterial community structure in the Po Valley, Italy, *Sci. Total*
679 *Environ.*, 593–594, 677–687, doi:10.1016/j.scitotenv.2017.03.199, 2017.
- 680 Jaenicke, R.: Atmospheric aerosols and global climate, *Journal of Aerosol Science*, 11(5), 577–588,
681 doi:10.1016/0021-8502(80)90131-7, 1980.
- 682 Joly, M., Amato, P., Sancelme, M., Vinatier, V., Abrantes, M., Deguillaume, L. and Delort, A.-M.:
683 Survival of microbial isolates from clouds toward simulated atmospheric stress factors, *Atmospheric*
684 *Environment*, 117, 92–98, doi:10.1016/j.atmosenv.2015.07.009, 2015.
- 685 Li, Y., Zheng, L., Zhang, Y., Liu, H. and Jing, H.: Comparative metagenomics study reveals pollution
686 induced changes of microbial genes in mangrove sediments, *Scientific Reports*, 9(1), 5739,
687 doi:10.1038/s41598-019-42260-4, 2019.



- 688 Malik, A. A., Chowdhury, S., Schlager, V., Oliver, A., Puissant, J., Vazquez, P. G. M., Jehmlich, N.,
689 von Bergen, M., Griffiths, R. I. and Gleixner, G.: Soil Fungal:Bacterial Ratios Are Linked to Altered
690 Carbon Cycling, *Front. Microbiol.*, 7, doi:10.3389/fmicb.2016.01247, 2016.
- 691 Oksanen, J., Guillaume Blanchet, F., Friendly, M., Kindt, R., Legendre, P., McGlenn, D., Minchin, P.
692 R., O'Hara, R. B., Simpson, G. L., Solymos, P., Stevens, M. H. H., Szoecs, E. and Wagner, H.:
693 Community Ecology Package, [online] Available from: <https://github.com/vegandevs/vegan>, 2019.
- 694 Rey, O., Danchin, E., Mirouze, M., Loot, C. and Blanchet, S.: Adaptation to Global Change: A
695 Transposable Element–Epigenetics Perspective, *Trends in Ecology & Evolution*, 31(7), 514–526,
696 doi:10.1016/j.tree.2016.03.013, 2016.
- 697 Shannan, S., Collins, K. and Emanuel, W. R.: Global mosaics of the standard MODIS land cover type
698 data, 2014.
- 699 Shoeb, E., Badar, U., Akhter, J., Shams, H., Sultana, M. and Ansari, M. A.: Horizontal gene transfer
700 of stress resistance genes through plasmid transport, *World J. Microbiol. Biotechnol.*, 28(3), 1021–
701 1025, doi:10.1007/s11274-011-0900-6, 2012.
- 702 Thomas, R. J., Webber, D., Hopkins, R., Frost, A., Laws, T., Jayasekera, P. N. and Atkins, T.: The
703 Cell Membrane as a Major Site of Damage during Aerosolization of *Escherichia coli*, *Appl. Environ.*
704 *Microbiol.*, 77(3), 920–925, doi:10.1128/AEM.01116-10, 2011.
- 705 Tignat-Perrier, R., Dommergue, A., Thollot, A., Keuschnig, C., Magand, O., Vogel, T. M. and
706 Larose, C.: Global airborne microbial communities controlled by surrounding landscapes and wind
707 conditions, *Sci Rep*, 9(1), 1–11, doi:10.1038/s41598-019-51073-4, 2019.
- 708 Tringe, S. G., von Mering, C., Kobayashi, A., Salamov, A. A., Chen, K., Chang, H. W., Podar, M.,
709 Short, J. M., Mathur, E. J., Detter, J. C., Bork, P., Hugenholtz, P. and Rubin, E. M.: Comparative
710 metagenomics of microbial communities, *Science*, 308(5721), 554–557, doi:10.1126/science.1107851,
711 2005.
- 712 Vaïtilingom, M., Amato, P., Sancelme, M., Laj, P., Leriche, M. and Delort, A.-M.: Contribution of
713 Microbial Activity to Carbon Chemistry in Clouds, *Appl Environ Microbiol*, 76(1), 23–29,
714 doi:10.1128/AEM.01127-09, 2010.
- 715 Vaïtilingom, M., Deguillaume, L., Vinatier, V., Sancelme, M., Amato, P., Chaumerliac, N. and Delort,
716 A.-M.: Potential impact of microbial activity on the oxidant capacity and organic carbon budget in
717 clouds, *PNAS*, 110(2), 559–564, doi:10.1073/pnas.1205743110, 2013.
- 718 Vartoukian, S. R., Palmer, R. M. and Wade, W. G.: Strategies for culture of 'unculturable' bacteria,
719 *FEMS Microbiology Letters*, 309(1), 1–7, doi:10.1111/j.1574-6968.2010.02000.x, 2010.
- 720 Wickham, H.: Flexibly Reshape Data: A Reboot of the Reshape Packa, [online] Available from:
721 <https://cran.r-project.org/web/packages/reshape2/reshape2.pdf>, 2017.
- 722 Wood, D. E. and Salzberg, S. L.: Kraken: ultrafast metagenomic sequence classification using exact
723 alignments, *Genome Biology*, 15(3), R46, doi:10.1186/gb-2014-15-3-r46, 2014.
- 724 Xie, W., Wang, F., Guo, L., Chen, Z., Sievert, S. M., Meng, J., Huang, G., Li, Y., Yan, Q., Wu, S.,
725 Wang, X., Chen, S., He, G., Xiao, X. and Xu, A.: Comparative metagenomics of microbial
726 communities inhabiting deep-sea hydrothermal vent chimneys with contrasting chemistries, *The*
727 *ISME Journal*, 5(3), 414–426, doi:10.1038/ismej.2010.144, 2011.
- 728 Yang, Y., Yokobori, S. and Yamagishi, A.: UV-resistant bacteria isolated from upper troposphere and
729 lower stratosphere, *Biol.Sci.Space*, 22, doi:10.2187/bss.22.18, 2008.



730 Yooseph, S., Neelson, K. H., Rusch, D. B., McCrow, J. P., Dupont, C. L., Kim, M., Johnson, J.,
731 Montgomery, R., Ferriera, S., Beeson, K., Williamson, S. J., Tovchigrechko, A., Allen, A. E., Zeigler,
732 L. A., Sutton, G., Eisenstadt, E., Rogers, Y.-H., Friedman, R., Frazier, M. and Venter, J. C.: Genomic
733 and functional adaptation in surface ocean planktonic prokaryotes, *Nature*, 468(7320), 60–66,
734 doi:10.1038/nature09530, 2010.

735 Yooseph, S., Andrews-Pfannkoch, C., Tenney, A., McQuaid, J., Williamson, S., Thiagarajan, M.,
736 Brami, D., Zeigler-Allen, L., Hoffman, J., Goll, J. B., Fadrosch, D., Glass, J., Adams, M. D., Friedman,
737 R. and Venter, J. C.: A Metagenomic Framework for the Study of Airborne Microbial Communities,
738 *PLOS ONE*, 8(12), e81862, doi:10.1371/journal.pone.0081862, 2013.

739 Zhang, H., Hu, Y., Zhou, C., Yang, Z., Wu, L., Zhu, M., Bao, H., Zhou, Y., Pang, M., Wang, R. and
740 Zhou, X.: Stress resistance, motility and biofilm formation mediated by a 25kb plasmid pLMSZ08 in
741 *Listeria monocytogenes*, *Food Control*, 94, 345–352, doi:10.1016/j.foodcont.2018.07.002, 2018.

742

743 **Competing interests.** The authors declare that they have no conflict of interest.

744

745 **Financial support.** This work was supported by the Agence Nationale de la Recherche
746 [ANR-15-CE01-0002–03 INHALE]; Région Auvergne-Rhône Alpes [ARC3 2016];
747 CAMPUS France [program XU GUANGQI] and the French Polar Institute IPEV [program
748 1028 and 399].

749

750 **Author contributions.** AD, CL and TMV designed the experiment. RTP, AD, AT and OM
751 conducted the sampling field campaign. RTP did the molecular biology, bioinformatics and
752 statistical analyses. RTP, AD, CL and TMV analyzed the results. RTP, TM, AD and CL wrote
753 the manuscript. All authors reviewed the manuscript.

754

755 **Acknowledgements.** The chemical analyses were performed at the IGE AirOSol platform. This
756 work was hosted by the following stations: Chacaltaya, Namco, puy de Dôme, Cape-Point, Pic-
757 du-Midi, Amsterdam-Island, Storm-Peak, Villum RS and we thank I.Jouvie, G.Hallar,
758 I.McCubbin, Benny and Jesper, B.Jensen, A.Nicosia, M.Ribeiro, L.Besaury, L.Bouvier,
759 M.Joly, I.Moreno, M.Rocca, F.Velarde for sampling and station management. We thank our
760 project partners: K.Sellegrì, P.Amato, M.Andrade, Q.Zhang, C.Labuschagne and L.Martin, J.
761 Sonke. We thank R.Edwards, J. Schauer and C.Worley for lending their HV sampler. We thank
762 L.Pouilloux for computing assistance and maintenance of the Newton server.

763

764 **Data availability.** Sequences reported in this paper have been deposited in ftp://ftp-adn.ec-lyon.fr/Tignat-Perrier_2020_air_metagen_INHALE/. A file has been attached explaining the
765 correspondence between file names and samples.
766